ARTICLE

Photoelectron Imaging Spectroscopy of ZrO^- Diatomic Anion†

Qing-yu Liu[a], Lian-rui Hu[b], Hui Chen[b*], Sheng-gui He[a*]

a. Beijing National Laboratory for Molecular Sciences, State Key Laboratory for Structural Chemistry of Unstable and Stable Species, Institute of Chemistry, Chinese Academy of Sciences, Beijing 100190, China

b. Beijing National Laboratory for Molecular Sciences, Key Laboratory of Photochemistry, Institute of Chemistry, Chinese Academy of Sciences, Beijing 100190, China

(Dated: Received on May 6, 2015; Accepted on July 5, 2015)

The diatomic ZrO^- anion has been prepared by laser ablation and studied by photoelectron imaging spectroscopy combined with quantum chemistry calculations. The observed photoelectron spectra can be well assigned on the basis of reported optical spectroscopy and high-level *ab initio* calculations. The ground state of ZrO^- is a $^2\Delta$ state with spin-orbit splitting of 578±12 cm^{-1}. The electron affinity of ZrO is 1.249±0.005 eV. For the first time, the $c^3\Sigma^-$ state of ZrO has been experimentally observed at 13316±24 cm^{-1} with respect to the $X^1\Sigma^+$ ground state. A comparison between ZrO and the isoelectronic molecule NbN has been made.

Key words: Diatomic molecules, Electronic structure, Spin-orbit splitting, Photoelectron imaging spectroscopy, *ab initio* calculations

I. INTRODUCTION

It is important to study electronic structures and reactivity of transition metal oxides that are important materials or species in research areas including catalysis, organometallic chemistry, surface science, superconductivity, and astrochemistry [1−10]. In particular, zirconium oxides are used in a variety of technological and commercial applications due to their high strength [11, 12] and high performance as catalysts or catalyst-supporting materials [13−18]. Diatomic metal oxides are the simplest systems to understand the chemical bonding and electronic structure of related materials. In this work, photoelectron imaging spectroscopy (PEIS) that has good resolution to resolve complex vibronic structures of transition metal species [2, 19, 20] is used to improve the understanding of the electronic structures of diatomic ZrO and ZrO^-.

The optical spectroscopy of ZrO has been extensively studied [21−25] and a strong driving force for this interest is that the ZrO spectrum is of the astrophysical significance [26−31]. The electronically ground state of ZrO is a singlet $^1\Sigma^+$. Ten electronically excited states (EESs) of ZrO were collected and summarized by Davis and Hammer in 1988 [21]. The microwave spectrum of ZrO was investigated by Jonsson in 1994 [22]. Heaven and co-workers studied the laser spectroscopy of ZrO in 1995 and accurate term energies for triplet states were determined [23]. The electric dipole moment of the $B^1\Pi$ state of ZrO was measured by Pettersson and co-workers in 2000 [24]. The laser induced fluorescence and dispersed fluorescence spectra of ZrO between 460 and 560 nm were studied by Balfour and Chowdhury in 2010 [25]. The experimentally determined EESs of ZrO below 15000 cm^{-1} are $a^3\Delta_1$ (1080 cm^{-1}), $a^3\Delta_2$ (1368 cm^{-1}), $a^3\Delta_3$ (1703 cm^{-1}), $A^1\Delta_2$ (5887 cm^{-1}), $b^3\Pi_0^-$ (11765 cm^{-1}), $b^3\Pi_0^+$ (11784 cm^{-1}), $b^3\Pi_1$ (12070 cm^{-1}), and $b^3\Pi_2$ (12427 cm^{-1}) [23]. These experimental results can be very well interpreted by the reliable *ab initio* calculations of Langhoff and Bauschlicher in 1990 [32] at the level of multi-reference configuration interaction (MRCI) and the calculated term values of $a^3\Delta$, $A^3\Delta$, and $b^3\Pi$ states are 1268, 5230, and 11566 cm^{-1}, respectively. The MRCI calculations predicted that the $c^3\Sigma^-$ of ZrO is at 13661 cm^{-1}. However, this level has never been addressed by optical spectroscopy although ZrO is among the most thoroughly studied transition metal diatomic oxides.

The optical (absorption/emission) spectroscopy has the high-resolution availability while it suffers from the dipole transition rule that allows transitions between electronic states with particular spin and orbital symmetries. Our previous PEIS study of MoC^- and NbN^- [19] indicated that many of the electronic states with very different symmetries could be reached at one excitation laser wavelength and the good resolution of the PEIS provides a chance to address the "dark" electronic states unvisited by optical spectroscopy. The PEIS of

†Dedicated to Professor Qing-shi Zhu on the occasion of his 70th birthday.

*Authors to whom correspondence should be addressed. E-mail: shengguihe@iccas.ac.cn, chenh@iccas.ac.cn

ZrO^- with 532 nm excitation were studied by Castleman and co-workers in 2010 to establish electronic state correlation between elements (such as Pd) and isoelectronic molecular counterparts (such as ZrO) [33]. Some observed bands in that work overlapped with each other and the assignments were made by assuming a $^2\Sigma^-$ ground state and two low-lying EESs of $^2\Delta_{3/2}$ and $^2\Delta_{5/2}$ for the ZrO^- anion. Bowen and co-workers studied the traditional photoelectron spectroscopy (PES) of ZrO^- with 355 nm excitation in 2012 and the assignments were made by assuming a $^2\Delta$ ground state of the anion [34]. In their assignments, the spin-orbit (SO) spitting of the $^2\Delta$ state ($^2\Delta_{3/2}$ and $^2\Delta_{5/2}$ components) of ZrO^- and the experimentally missing $c^3\Sigma^-$ state of ZrO predicted at 13661 cm^{-1} by the MRCI calculations [32] were not considered. In this work, by using a wavelength tunable laser, we provide improved PE spectra to address the $c^3\Sigma^-$ state of ZrO and the ground state of ZrO^-.

II. METHODS

A. Experimental methods

The details of the experimental setup can be found in our previous study [19], and only a brief outline of the experiments is given below. The zirconium oxide anions were generated by pulsed laser ablation of a rotating and translating metal disk in the presence of about 0.03% O_2 seeded in a He carrier gas (99.999%) with a backing pressure of 8 atm. The generated anions passed through two identical reflectors with Z-shaped configuration in a time-of-flight mass spectrometer (TOF-MS) and then the ZrO^- ions were selected by a mass gate to interact with a wavelength-tunable laser (Continuum OPO, Horizon I) of which the wavelengths were determined using a grating spectrograph (Acton SpectraPro 500I) calibrated with atomic spectral lines of a mercury-argon lamp [35]. The photo-detached electrons were accelerated and focused by pulsed-electric potential to a detection system with two micro-channel places and one phosphor screen on which the electron positions were imaged with a charge-coupled device (CCD) camera. The images were transferred into a computer for averaging (by 20000−50000 laser shots) and inverse-Abel transformation of the two-dimensional (2D) images into three-dimensional (3D) electron distributions as described in Ref.[36]. The photo-electron kinetic energies were calibrated with the known electron detachment energies of gold anions [37]. The precision of the electron detachment energies for narrow and unblended bands is better than ±3 meV.

In addition to the photoelectron kinetic energies, the photoelectron angular distribution (PAD) [38] can also be derived from the experimental images of the CCD camera and provides additional information for the symmetries of the involved electronic states. For one-photon detachment, the photoelectron angular distribution (PAD) is given by [38]:

$$I(\theta) \sim [1 + \beta P_2(\cos\theta)] \quad (1)$$

$$P_2(\cos\theta) = \frac{1}{2}(3\cos^2\theta - 1) \quad (2)$$

in which θ is the angle between the direction of the ejected electron and the polarization direction of the detachment laser, and P_2 is the second order Legendre polynomial. The anisotropy parameter, β, is encoded with information quantifying the degree of alignment between the direction of the photo-detached electrons and the laser polarization direction, and it is numerically confined as $-1 \le \beta \le 2$. To satisfy the dipole selection rule, $\Delta l = \pm 1$, the electron detachment from s-type (l=0) atomic orbital (AO) generate one type (s→p, l=0+1) of outgoing partial wave with maximum intensity parallel to the laser polarization direction and β=2. The electron detachment from other AO (such as p or d) can generate two types (such as p→s and p→d; or d→p and d→f) of outgoing partial waves and their pure interference can result in β=−1. Without inferences, the p→s, p→d, d→p, and d→f partial waves have the β parameters ranging from 0 to 1. In molecular system, the photoelectron angular distributions can be obtained by calculating the overlap integration of the initial and final wavefunction based on molecular orbitals (MOs) [39, 40].

B. Theoretical methods

The *ab initio* calculations using Gaussian 09 program [41] have been carried out to investigate the ground state structures and energies of ZrO^- and ZrO. The coupled-cluster method with single, double, and perturbative triple excitations method (CCSD(T)) [42, 43] was used. The aug-cc-pwCVQZ-PP basis set [44] for Zr and aug-cc-pVQZ basis set [45] for O were adopted. The 4s4p electrons of Zr were correlated in all the coupled-cluster calculations. Meanwhile, the scalar relativistic effect was taken into account using the Stuttgart new relativistic energy-consistent small-core pseudopotential (PP) ECP28MDF in combination with the above basis set for Zr [44]. The bond lengths of the diatomic systems were scanned to get the minimum energies. To calculate the SO splitting of the $^2\Delta$ states ($^2\Delta_{3/2}$ and $^2\Delta_{5/2}$ components) of the ZrO^- anion, the MRCISD calculation [46] with Molpro program package [47] were performed. The basis sets and pseudopotentials used was the same as those in the CCSD(T) calculations. The 4s4p electrons of Zr were correlated in all the MRCISD calculations. The MRCISD and the preceding complete active space self-consistent field (CASSCF) calculations employed an active space composed of full valence shells of Zr and O atoms. This resultant active space is thus 11 electrons distributed in 10 orbitals, labeled as (11e, 10o). The SO coupling effect was included using a contracted SO configuration interaction method

DOI:10.1063/1674-0068/28/cjcp1505090

TABLE I Observed binding energies, β parameters, and assignments.

Label	BE/eV	β (λ/nm)	Assignments		Upper state E/cm^{-1}	
			Electronic	Vibrational	This work	Reference
hb_1	1.142		$^1\Sigma_0^+\leftarrow{}^2\Delta_{3/2}$	0←1		
α	1.179	1.0 (925)	$^1\Sigma_0^+\leftarrow{}^2\Delta_{5/2}$	0←0	−20[a]	
X	1.249	0.9 (925)	$^1\Sigma_0^+\leftarrow{}^2\Delta_{3/2}$	0←0	−33	0
hb_2	1.280	1.2 (925)	$^3\Delta_1\leftarrow{}^2\Delta_{3/2}$	0←1		
β_1	1.314	0.3 (925)	$^3\Delta_1\leftarrow{}^2\Delta_{5/2}$	0←0	1069[a]	
	1.314	1.3 (700)	$^3\Delta_1\leftarrow{}^2\Delta_{5/2}$	0←0	1069[a]	
β_2	1.349	1.6 (700)	$^3\Delta_2\leftarrow{}^2\Delta_{5/2}$	0←0	1351[a]	
a_1	1.387	1.7 (700)	$^3\Delta_1\leftarrow{}^2\Delta_{3/2}$	0←0	1080[b]	1080 [23]
a_2	1.421	1.5 (700)	$^3\Delta_2\leftarrow{}^2\Delta_{3/2}$	0←0	1354	1368 [23]
a_3	1.507	1.5 (700)	$^3\Delta_1\leftarrow{}^2\Delta_{3/2}$	1←0	2048	
a_4	1.534	1.5 (700)	$^3\Delta_2\leftarrow{}^2\Delta_{3/2}$	1←0	2266	
γ_1	1.915	2.0 (500)	$^1\Delta_2\leftarrow{}^2\Delta_{5/2}$	0←0	5917[a]	
A_1	1.985	1.9 (500)	$^1\Delta_2\leftarrow{}^2\Delta_{3/2}$	0←0	5903	5887 [23]
γ_2	2.034	1.6 (500)	$^1\Delta_2\leftarrow{}^2\Delta_{5/2}$	1←0	6877[a]	
A_2	2.105	1.7 (500)	$^1\Delta_2\leftarrow{}^2\Delta_{3/2}$	1←0	6871	
b_1	2.716	0.5 (500)	$^3\Pi_0^-\leftarrow{}^2\Delta_{3/2}$	0←0	11800	11765 [23]
	2.716	0.5 (500)	$^3\Pi_0^+\leftarrow{}^2\Delta_{3/2}$	0←0	11800	11784 [23]
b_2	2.750	0.3 (500)	$^3\Pi_1\leftarrow{}^2\Delta_{3/2}$	0←0	12074	12070 [23]
δ	2.831	0.2 (500)	$^3\Sigma^-\leftarrow{}^2\Delta_{5/2}$	0←0	13305[a]	
c	2.904	0.4 (500)	$^3\Sigma^-\leftarrow{}^2\Delta_{3/2}$	0←0	13316	13661 [32]

[a] The term value of the $X^2\Delta_{5/2}$ state is set to 578 cm^{-1}.
[b] Set to the value by optical spectroscopy [23].

[48] with two-component SO PPs [44] on transition metals. Only two degenerate $^2\Delta$ states were included in the SO coupling state-interacting calculations. The SO coupling matrix was constructed on a basis of the MRCISD state-specific scalar relativistic states. The matrix was then diagonalized to obtain the SO states and energies.

III. RESULTS

A. Experimental results

The PE images and the transformed spectra of ZrO^- in terms of electron binding energy (BE) at four typical excitation laser wavelengths are shown in Fig.1. The observed BEs and the β parameters are collected in Table I. At 700 nm excitation (Fig.1(b)), four relatively strong bands marked as a_1−a_4 are located at the higher-BE side and additional weak bands are at the lower-BE side. These weak bands can be well resolved at 925 nm excitation (Fig.1(a)). The pattern (band intensity and spacing) of the a_1-a_4 bands of ZrO^- is very similar to that of the X_1-X_4 bands observed for NbN^- (Fig.1(b) inset) in our previous study [19]. The ZrO^- and NbN^- are isoelectronic systems and the $X_{1,2}$ and $X_{3,4}$ bands of NbN^- were assigned as $^3\Delta_{1,2}\leftarrow{}^2\Delta_{3/2}$ (0←0) and $^2\Delta_{1,2}\leftarrow{}^3\Delta_{3/2}$ (1←0), respectively. As a result, similar assignments were made for the a_1-a_4 bands of ZrO^- (Table I). Such assignments are also consistent with the results by optical spectroscopy: (i) the a_2-a_1 distance is 274±24 cm^{-1} which agrees with the $a^3\Delta_2/a^3\Delta_1$ splitting (288 cm^{-1}) [23] and (ii) the a_3-a_1 distance is 968±24 cm^{-1} which reasonably agrees with the reported vibrational frequency of the $a^3\Delta$ state (938 cm^{-1}) [31].

Similar to the $X^3\Delta$ state of NbN^-, the $a^3\Delta$ state of ZrO^- has the electron configuration of $(3\sigma)^2(1\delta)^1$. The β parameters of the a_1-a_4 bands (1.5−1.7, see Table I) are quite large, suggesting that these bands are due to s-type ($(3\sigma)^1(1\delta)^1\leftarrow(3\sigma)^2(1\delta)^1$) rather than d-type ($(3\sigma)^1(1\delta)^1\leftarrow(3\sigma)^1(1\delta)^2$) excitation. Because the a_1 transition (1.387±0.003 eV) is very strong, it must be a cold band rather than a hot band. As a result, the electronically ground state of ZrO^- can be confirmed to be the $^2\Delta$ state ($(3\sigma)^2(1\delta)^1$) rather than the $^2\Sigma$ state ($(3\sigma)^1(1\delta)^2$).

Once the strongest a_1-a_4 bands are assigned, it is straightforward to assign a few more bands on the basis of the well determined term values by optical spectroscopy [23]. With respect to the $X^1\Sigma^+$ ground state $(3\sigma)^2$ of ZrO, the term value of the $a^3\Delta_1$ state is 1080 cm^{-1}, which matches the distance (1113±40 cm^{-1}) between the a_1 band (Fig.1(b)) and the X band (Fig.1(a)). As a result, the X band lo-

DOI:10.1063/1674-0068/28/cjcp1505090

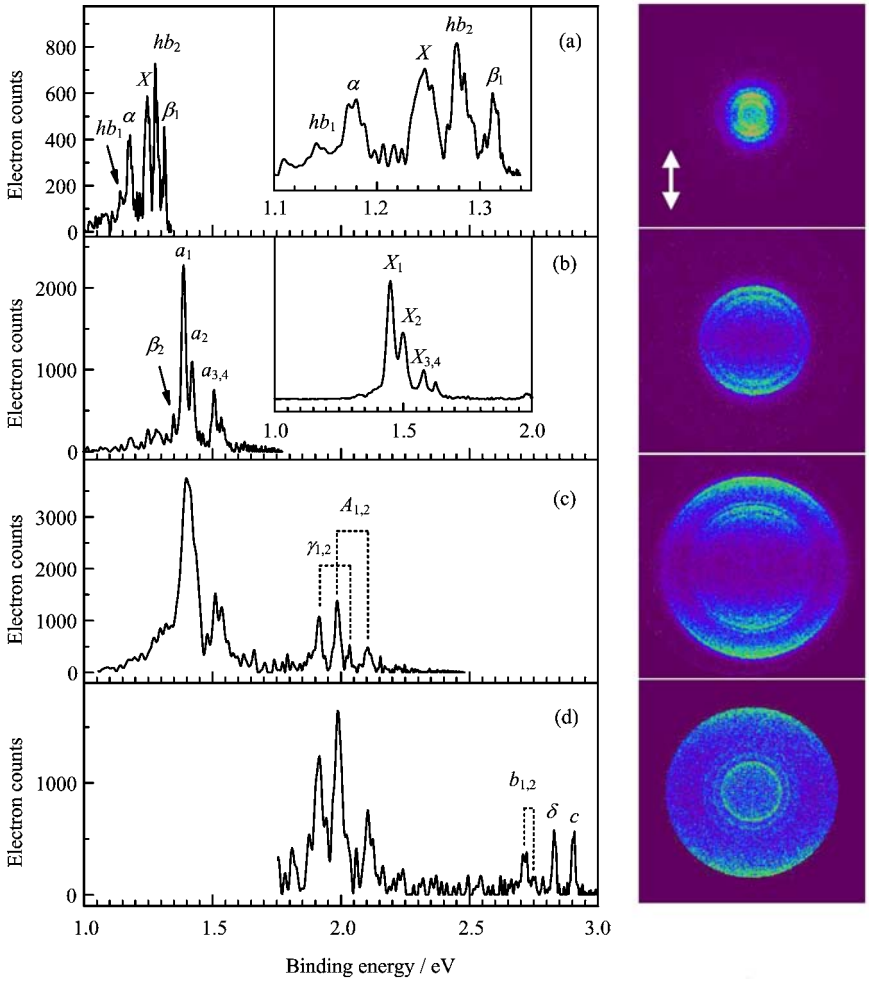

FIG. 1 Photoelectron images and spectra of ZrO^- taken at (a) 925 nm, (b) 700 nm, (c) 500 nm, and (d) 410 nm. The inset in (a) shows the expanded spectrum of (a). The inset in (b) shows a portion of the NbN^- spectrum taken at 550 nm in Ref.[19].

cated at 1.249±0.005 eV is the electron affinity (EA) defining transition of ZrO ($X^1\Sigma^+\leftarrow X^3\Delta_{3/2}$). With respect to the $a^3\Delta_1$ state of ZrO, the term value of the $A^1\Delta_2$ state is 4807 cm^{-1}, which matches the distance (4823±24 cm^{-1}) between the A_1 band (Fig.1(c)) and the a_1 band (Fig.1(b)). As a result, the A_1 band located at 1.985±0.003 eV is assigned as $A^1\Delta_2\leftarrow X^2\Delta_{3/2}$. Similarly, the weak b_1 and b_2 bands observed at 410 nm excitation (Fig.1(d)) can be assigned as $b^3\Pi_0\leftarrow X^2\Delta_{3/2}$ and $b^3\Pi_1\leftarrow X^2\Delta_{3/2}$, respectively.

At 500 nm excitation, a band marked as γ_1 is present on the left side of the A_1 band ($A^1\Delta_2\leftarrow X^2\Delta_{3/2}$) (Fig.1(c)). The A_1-γ_1 distance is only 565±24 cm^{-1}, which is too small to be considered as the vibrational frequency of the ZrO^- anion, *i.e.*, the γ_1 band can not be assigned as the vibrational hot band of the A_1 transition. It turns out that the 565±24 cm^{-1} distance appears several times in the PE spectra: $X-\alpha$=565 cm^{-1}, $a_1-\beta_1$=589 cm^{-1}, $a_2-\beta_2$=581 cm^{-1}, and $c-\delta$=589 cm^{-1}. As a result, a low-lying excited state of ZrO^- can be located at 578±12 cm^{-1} with respect to the $X^2\Delta_{3/2}$ state. This state at 578±12 cm^{-1} is assigned as the $X^2\Delta_{5/2}$, the other SO component of the $X^2\Delta$ state. This assignment is further supported by the fact that each of the X/α, a_1/β_1, a_2/β_2, A_1/γ_1, and c/δ couples have similar β parameters under the same excitation laser wavelength. In addition, the quantum chemistry calculations have also predicted a similar SO splitting for the $X^2\Delta$ state of ZrO^- (see computational results below).

At 925 nm excitation, the two remaining band marked as hb_1 and hb_2 can then be assigned as the vibrational hot bands of the X and a_1 transitions, respectively (Fig.1(a)). The vibrational frequency of ZrO^- $X^2\Delta_{3/2}$ state is determined to be 863±24 cm^{-1}. At 500 nm excitation (Fig.1(c)), the two remaining bands marked as γ_2 and A_2 are related to the vibrational excitations of ZrO $A^2\Delta_2$ (v=1) state. The last two unassigned bands (Fig.1(d)) are the δ and c bands that own the same neutral state and two anion states ($X^2\Delta_{5/2}$

DOI:10.1063/1674-0068/28/cjcp1505090

TABLE II Comparison between theory and experiment for the bond lengths (r_e) and relative energies (E_r) of ZrO and ZrO^-.

	r_e/pm		E_r/eV	
	Theory	Expt.	Theory	Expt.
ZrO^- ($X^2\Delta_{3/2}$)	176.5		0	0
ZrO^- ($X^2\Delta_{5/2}$)	176.5		0.079	0.071
ZrO ($X^1\Sigma^+$)	171.5	171.2 [49]	1.153	1.247
ZrO ($a^3\Delta$)	173.0	172.9 [49]	1.330	1.388

and $X^2\Delta_{3/2}$). The term value of the neutral state can be determined to be 13316±24 cm^{-1}. This value does not match any term values of ZrO determined by optical spectroscopy [21, 23, 25], while it matches the term value of the $c^3\Sigma^-$ state predicted by the MRCI calculations (13661 cm^{-1}). As a result, the δ and c bands are assigned as $c^3\Sigma^- \leftarrow X^2\Delta_{5/2}$ and $c^3\Sigma^- \leftarrow X^2\Delta_{3/2}$, respectively (Table I).

B. Computational results

The computational results of this study are listed in Table II, in which available experimental results [49] are also given for a comparison. The CCSD(T) calculations correctly predicted that for the neutral ZrO, the triplet state ($^3\Delta$, $(3\sigma)^1(1\delta)^1$) is slightly above the singlet state ($^1\Sigma^+$, $(3\sigma)^2$). The calculated $a^3\Delta/X^1\Sigma^+$ energy difference is 1129 cm^{-1} (0.140 eV), in agreement with the experimental value of 1392 cm^{-1} (the average of the term values of $a^3\Delta_1$ (1080 cm^{-1}) and $a^3\Delta_3$ (1703 cm^{-1})) [23]. The experimental bond lengths of ZrO ($X^1\Sigma^+$ and $a^3\Delta$) can be well reproduced (within 0.3 pm) by the CCSD(T) calculations.

The CCSD(T) calculations predicted that the ground state of the ZrO^- anion is a $^2\Delta$ state with electron configuration of $(3\sigma)^2(1\delta)^1$. The result is very well in agreement with the result of the imaging spectroscopy in this study (spectral pattern as well as β parameters of the a_1−a_4 peaks in Fig.1(b)). The experimental EA value of ZrO (1.249±0.005 eV) is well reproduced by the calculations (1.153 eV). The SO splitting of the anion $X^2\Delta$ state ($^2\Delta_{5/2}/^2\Delta_{3/2}$) was calculated to be 79.5 meV (641 cm^{-1}) in good agreement with the experimental value (71.7 meV, 578±12 cm^{-1}).

IV. DISCUSSION

The PE spectra of ZrO^- were reported previously [33, 34]. The resolution of the PEIS in this study is good enough to resolve and then correctly assign the SO splittings of ZrO ($a^2\Delta_2/a^2\Delta_1$) and ZrO^- ($X^2\Delta_{5/2}/X^2\Delta_{3/2}$). The term values from the PEIS can then be compared with those from optical spectroscopy (Table I, the last two columns). The $c^3\Sigma^-$ state of ZrO

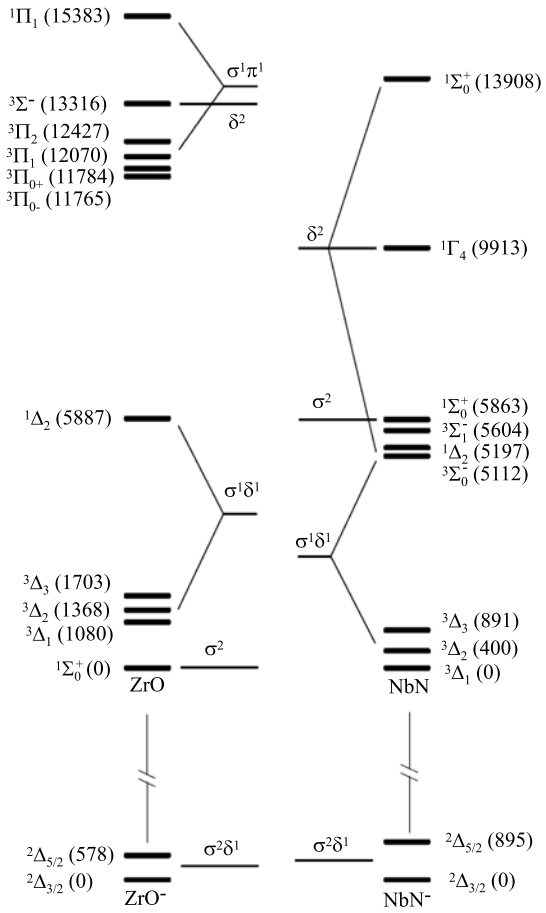

FIG. 2 Comparison of the electron configurations and energy levels of ZrO (left) versus NbN (right). The left part of this figure was made on the basis of the data in Table I while the right part was adapted from Ref.[19].

(13316±24 cm^{-1}) was experimentally addressed for the first time although the ZrO is among the most thoroughly studied transition metal diatomic oxides.

As summarized in left part of Fig.2, the experimentally observed PEI bands (Fig.1) are mainly due to many possible fillings of two electrons into three different types of valence MOs: (i) σ-type MO (3σ) characterized with Zr5s AO, (ii) δ-type MO (1δ) that is essentially the metal $4d_{xy}$ or $4d_{x^2-y^2}$ AO, and (iii) π-type MO (1π) characterized with O2p and Zr4d AOs. The right part of Fig.2 shows the electron configurations and energy levels of the isoelectronic molecule NbN and its anion NbN^- [19, 50, 51] in order to have a comparison. For ZrO molecule, the ground state has the σ^2 electron configuration while the $\sigma^1\delta^1$ configuration is less stable. In contrast, the relative stability of σ^2 versus $\sigma^1\delta^1$ switches in the case of NbN: the $\sigma^1\delta^1$ configuration becomes more stable. This is due to the fact that the heavier 4d metal atoms have apparently increased stability of the 4d orbitals [52, 53]. The increased stability of Nb4d over Zr4d orbitals results in much lower energy of the NbN $^3\Sigma^-$ level (δ^2, 5112 and 5604 cm^{-1})

DOI:10.1063/1674-0068/28/cjcp1505090

than that of the ZrO $^3\Sigma^-$ level (δ^2, 13316 cm^{-1}). It is noteworthy that the $^3\Sigma^-$ level (δ^2) becomes the ground state of MoC due to further stability of the Mo4d orbital [19].

Although there is rather big difference between the relative stability of the electron configurations when ZrO is compared with NbN, these two isoelectronic systems do have similarities in terms of energy level splitting and spectral pattern. For example, for the $\sigma^1\delta^1$ configuration, the $^1\Delta_2/^3\Delta_2$ splitting of ZrO (4519 cm^{-1}) is very close to that of NbN (4797 cm^{-1}). Both of the molecules have the same anion ground state ($\sigma^2\delta^1$, $^2\Delta$). The spectral pattern for the $^3\Delta_{1,2}\leftarrow{}^2\Delta_{3/2}$ (0, 1←0) transitions of ZrO and NbN systems are very similar to each other (Fig.1(b)). Because lighter metal atoms have smaller atomic SO parameters [54], the SO splittings of the ZrO $a^3\Delta_2/a^3\Delta_1$ (288 cm^{-1}) and $a^3\Delta_3/a^3\Delta_2$ (335 cm^{-1}) are smaller than those of the NbN $X^3\Delta_2/X^3\Delta_1$ (400 cm^{-1}) and $X^3\Delta_3/X^3\Delta_2$ (491 cm^{-1}). This also rationalizes the smaller SO splitting of ZrO^- $X^2\Delta$ state ($^2\Delta_{5/2}/^2\Delta_{3/2}$=578 cm^{-1}) than that of NbN^- $X^2\Delta$ state ($^2\Delta_{5/2}/^2\Delta_{3/2}$=895 cm^{-1}).

V. CONCLUSION

Photoelectron imaging spectroscopy of ZrO^- has been studied. Seven electronic levels $X^1\Sigma_0^+$, $a^3\Delta_1$, $X^3\Delta_2$, $A^1\Delta_1$, $b^3\Pi_0$, $b^3\Pi_1$, and $c^3\Sigma^-$ of ZrO have been reached by the imaging spectroscopy and the assignments were very well supported by literature reported optical spectroscopy and high-level *ab initio* calculations. The $c^3\Sigma^-$ state at 13316±24 cm^{-1} is experimentally addressed for the first time in this study. The ground state of the ZrO^- anion is a $^2\Delta$ state rather than a $^2\Sigma$ state. The spin-orbit splitting of the anion $X^2\Delta$ state ($^2\Delta_{5/2}/^2\Delta_{3/2}$) has been determined to be 578±12 cm^{-1}. The electron affinity of ZrO is 1.249±0.005 eV. The strongest band observed at 1.387±0.003 eV is due to the $a^3\Delta_1\leftarrow X^2\Delta_{3/2}$ transition. The vibrational frequency of the ZrO^- ground state is 863±24 cm^{-1}. When the ZrO is compared with the isoelectronic molecule NbN, the increased stability of Nb4d orbitals over Zr4d changes the energy ordering of $(1\delta)^2>(3\sigma)^1(1\delta)^1>(3\sigma)^2$ for ZrO to $(1\delta)^2>(3\sigma)^2>(3\sigma)^1(1\delta)^1$ for NbN.

VI. ACKNOWLEDGMENTS

This work was supported by the Chinese Academy of Sciences (No.YZ201318), the National Natural Science Foundation of China (No.21325314), and the Major Research Plan of China (No.2013CB834603).

[1] Y. Gong, M. F. Zhou, and L. Andrews, Chem. Rev. **109**, 6765 (2009).
[2] J. B. Kim, M. L. Weichman, and D. M. Neumark, J. Am. Chem. Soc. **136**, 7159 (2014).
[3] Y. X. Zhao, X. N. Wu, J. B. Ma, S. G. He, and X. L. Ding, Phys. Chem. Chem. Phys. **13**, 1925 (2011).
[4] X. L. Ding, X. N. Wu, Y. X. Zhao, and S. G. He, Acc. Chem. Res. **45**, 382 (2012).
[5] Q. Y. Liu and S. G. He, Chem. J. Chin. Univ. Chin. **35**, 665 (2014).
[6] H. Schwarz, Isr. J. Chem. **54**, 1413 (2014).
[7] S. Yin and E. R. Bernstein, Int. J. Mass Spectrom. **321/322**, 49 (2012).
[8] Z. Luo and A. W. Castleman, Acc. Chem. Res. **47**, 2931 (2014).
[9] K. R. Asmis, Phys. Chem. Chem. Phys. **14**, 9270 (2012).
[10] H. J. Zhai, Q. Chen, H. Bai, S. D. Li, and L. S. Wang, Acc. Chem. Res. **47**, 2435 (2014).
[11] M. V. Ganduglia-Pirovano, A. Hofmann, and J. Sauer, Surf. Sci. Rep. **62**, 219 (2007).
[12] G. Jomard, T. Petit, A. Pasturel, L. Magaud, G. Kresse, and J. Hafner, Phys. Rev. B **59**, 4044 (1999).
[13] J. Zhu, J. G. Van Ommen, H. J. M. Bouwmeester, and L. Lefferts, J. Catal. **233**, 434 (2005).
[14] J. Zhu, J. G. Van Ommen, and L. Lefferts, Catal. Today **112**, 82 (2006).
[15] G. Jin, G. Lu, Y. Guo, J. Wang, and X. Liu, Catal. Today **93-95**, 173 (2004).
[16] M. Kotobuki, R. Leppelt, D. A. Hansgen, D. Widmann, and R. J. Behm, J. Catal. **264**, 67 (2009).
[17] D. Widmann, Y. Liu, F. Schüth, and R. J. Behm, J. Catal. **276**, 292 (2010).
[18] D. Widmann and R. J. Behm, Angew. Chem. Int. Ed. **50**, 10241 (2011).
[19] Q. Y. Liu, L. Hu, Z. Y. Li, C. G. Ning, J. B. Ma, H. Chen, and S. G. He, J. Chem. Phys. **142**, 164301 (2015).
[20] H. T. Liu, D. L. Huang, Y. Liu, L. F. Cheung, P. D. Dau, C. G. Ning, and L. S. Wang, J. Phys. Chem. Lett. 637 (2015).
[21] S. P. Davis and P. D. Hammer, Astrophys. J. **332**, 1090 (1988).
[22] J. Jonsson, J. Mol. Spectrosc. **167**, 42 (1994).
[23] L. A. Kaledin, J. E. McCord, and M. C. Heaven, J. Mol. Spectrosc. **174**, 93 (1995).
[24] A. Pettersson, R. Koivisto, B. Lindgren, C. Lundevall, P. Royen, U. Sassenberg, and W. Shi, J. Mol. Spectrosc. **200**, 65 (2000).
[25] W. J. Balfour and P. K. Chowdhury, Chem. Phys. Lett. **485**, 8 (2010).
[26] P. D. Hammer, S. P. Davis, and A. C. Zook, J. Chem. Phys. **74**, 5320 (1981).
[27] P. D. Hammer and S. P. Davis, Astrophys. J. Suppl. Ser. **47**, 201 (1981).
[28] J. G. Phillips and S. P. Davis, Astrophys. J. Suppl. Ser. **32**, 537 (1976).
[29] J. G. Phillips and S. P. Davis, Astrophys. J. **206**, 632 (1976).
[30] J. G. Phillips, S. P. Davis, and D. C. Galehouse, Astrophys. J. **234**, 401 (1979).
[31] P. D. Hammer and S. P. Davis, Astrophys. J. **237**, L51

DOI:10.1063/1674-0068/28/cjcp1505090

(1980).
[32] S. R. Langhoff and C. W. Bauschlicher, Astrophys. J. **349**, 369 (1990).
[33] S. J. Peppernick, K. D. D. Gunaratne, and A. W. Castleman, Proc. Natl. Acad. Sci. USA **107**, 975 (2010).
[34] X. Li, W. Zheng, A. Buonaugurio, A. Buytendyk, K. Bowen, and K. Balasubramanian, J. Chem. Phys. **136**, 154306 (2012).
[35] B. Xu, Y. X. Zhao, X. L. Ding, Q. Y. Liu, and S. G. He, J. Phys. Chem. A **117**, 2961 (2013).
[36] V. Dribinski, A. Ossadtchi, V. A. Mandelshtam, and H. Reisler, Rev. Sci. Instrum. **73**, 2634 (2002).
[37] X. Wu, Z. B. Qin, H. Xie, X. H. Wu, R. Cong, and Z. C. Tang, Chin. J. Chem. Phys. **23**, 373 (2010).
[38] A. Sanov, Annu. Rev. Phys. Chem. **65**, 341 (2014).
[39] D. Dill, J. Chem. Phys. **65**, 1130 (1976).
[40] C. M. Oana and A. I. Krylov, J. Chem. Phys. **131**, 124114 (2009).
[41] M. J. Frisch, G. W. Trucks, H. B. Schlegel, G. E. Scuseria, M. A. Robb, J. R. Cheeseman, G. Scalmani, V. Barone, B. Mennucci, G. A. Petersson, H. Nakatsuji, M. Caricato, X. Li, H. P. Hratchian, A. F. Izmaylov, J. Bloino, G. Zheng, J. L. Sonnenberg, M. Hada, M. Ehara, K. Toyota, R. Fukuda, J. Hasegawa, M. Ishida, T. Nakajima, Y. Honda, O. Kitao, H. Nakai, T. Vreven, J. A. Jr. Montgomery, J. E. Peralta, F. Ogliaro, M. Bearpark, J. J. Heyd, E. Brothers, K. N. Kudin, V. N. Staroverov, R. Kobayashi, J. Normand, K. Raghavachari, A. Rendell, J. C. Burant, S. S. Iyengar, J. Tomasi, M. Cossi, N. Rega, J. M. Millam, M. Klene, J. E. Knox, J. B. Cross, V. Bakken, C. Adamo, J. Jaramillo, R. Gomperts, R. E. Stratmann, O. Yazyev, A. J. Austin, R. Cammi, C. Pomelli, J. W. Ochterski, R. L. Martin, K. Morokuma, V. G. Zakrzewski, G. A. Voth, P. Salvador, J. J. Dannenberg, S. Dapprich, A. D. Daniels, Ö. Farkas, J. B. Foresman, J. V. Ortiz, J. Cioslowski, and D. J. Fox, *Gaussian 09, Revision A.1*, Wallingford CT: Gaussian, Inc., (2009).
[42] K. Raghavachari, G. W. Trucks, J. A. Pople, and M. Head-Gordon, Chem. Phys. Lett. **157**, 479 (1989).
[43] J. D. Watts, J. Gauss, and R. J. Bartlett, J. Chem. Phys. **98**, 8718 (1993).
[44] K. A. Peterson, D. Figgen, M. Dolg, and H. Stoll, J. Chem. Phys. **126**, 124101 (2007).
[45] T. H. Jr. Dunning, J. Chem. Phys. **90**, 1007 (1989).
[46] H. J. Werner and P. J. Knowles, J. Chem. Phys. **89**, 5803 (1988).
[47] H. J. Werner, P. J. Knowles, F. R. Manby, M. Schütz, P. Celani, G. Knizia, T. Korona, R. Lindh, A. Mitrushenkov, G. Rauhut, T. B. Adler, R. D. Amos, A. Bernhardsson, A. Berning, D. L. Cooper, M. J. O. Deegan, A. J. Dobbyn, F. Eckert, E. Goll, C. Hampel, A. Hesselmann, G. Hetzer, T. Hrenar, G. Jansen, C. Köppl, Y. Liu, A. W. Lloyd, R. A. Mata, A. J. May, S. J. McNicholas, W. Meyer, M. E. Mura, A. Nicklass, P. Palmieri, K. Pflüger, R. Pitzer, M. Reiher, T. Shiozaki, H. Stoll, A. J. Stone, R. Tarroni, T. Thorsteinsson, M. Wang, and A. Wolf, *MOLPRO, Version 2010.1, a Package of ab initio Programs*, http://www.molpro.net.
[48] A. Berning, M. Schweizer, H. J. Werner, P. J. Knowles, and P. Palmieri, Mol. Phys. **98**, 1823 (2000).
[49] K. P. Huber and G. Herzberg, *Molecular Spectra and Molecular Structure IV. Constants of Diatomic Molecules*, Princeton: Van Nostrand, (1979).
[50] R. S. Ram and P. F. Bernath, J. Mol. Spectrosc. **201**, 267 (2000).
[51] Y. Azuma, G. Huang, M. P. J. Lyne, A. J. Merer, and V. I. Srdanov, J. Chem. Phys. **100**, 4138 (1994).
[52] D. J. Brugh, T. J. Ronningen, and M. D. Morse, J. Chem. Phys. **109**, 7851 (1998).
[53] S. R. Langhoff and C. W. Bauschlicher, J. Mol. Spectrosc. **143**, 169 (1990).
[54] M. Vijayakumar and M. S. Gopinathan, Theochem. J. Mol. Struct. **361**, 15 (1996).

DOI:10.1063/1674-0068/28/cjcp1505090